PROCEEDINGS OF SPIE

High performance incandescent lighting using a selective emitter and nanophotonic filters

Arny Leroy, Bikram Bhatia, Kyle Wilke, Ognjen Ilic, Marin Soljačić, et al.

SPIE.

High performance incandescent lighting using a selective emitter and nanophotonic filters

Arny Leroy[*a], Bikram Bhatia[a], Kyle Wilke[a], Ognjen Ilic[b], Marin Soljačić[c,d], Evelyn N. Wang[a]

[a]Device Research Laboratory, Department of Mechanical Engineering, Massachusetts Institute of Technology, 77 Massachusetts Avenue, Cambridge, Massachusetts 02139, USA; [b]Department of Applied Physics and Materials Science, California Institute of Technology, 1200 East California Boulevard, Pasadena, California 91125, USA; [c]Research Laboratory of Electronics, Massachusetts Institute of Technology, 77 Massachusetts Avenue, Cambridge, Massachusetts 02139, USA; [d]Institute for Soldier Nanotechnology, Massachusetts Institute of Technology, 77 Massachusetts Avenue, Cambridge, Massachusetts 02139, USA

ABSTRACT

Previous approaches for improving the efficiency of incandescent light bulbs (ILBs) have relied on tailoring the emitted spectrum using cold-side interference filters that reflect the infrared energy back to the emitter while transmitting the visible light. While this approach has, in theory, potential to surpass light-emitting diodes (LEDs) in terms of luminous efficiency while conserving the excellent color rendering index (CRI) inherent to ILBs, challenges such as low view factor between the emitter and filter, high emitter (>2800 K) and filter temperatures and emitter evaporation have significantly limited the maximum efficiency. In this work, we first analyze the effect of non-idealities in the cold-side filter, the emitter and the view factor on the luminous efficiency. Second, we theoretically and experimentally demonstrate that the loss in efficiency associated with low view factors can be minimized by using a selective emitter (e.g., high emissivity in the visible and low emissivity in the infrared) with a filter. Finally, we discuss the challenges in achieving a high performance and long-lasting incandescent light source including the emitter and filter thermal stability as well as emitter evaporation.

Keywords: Incandescent lighting, selective emitter, selective filter, nanophotonic filters, thermal stability, emitter evaporation

1. INTRODUCTION

It is estimated[1] that around $34 billion were spent in 2016 on electricity for lighting in the residential and commercial sectors in the United States. Despite incandescent light bulbs (ILBs) being much less efficient than light-emitting diodes (LEDs), they were still found in 82%[2] of households in the United States in 2015 as opposed to 28% for LEDs. ILBs, although inefficient due to dominant emission at infrared wavelengths, are cheap and offer the best possible color rendering index (CRI; metric of how faithfully a light source reproduces colors of an illuminated object in comparison to an ideal light source such as a blackbody or the sun) of 100, superior to any other light source in terms of quality of light. In comparison, more expensive LEDs with luminous efficiencies (metric of how efficiently a light source produces visible light, as specified by the human eye sensitivity curve[3]) five to ten times higher than ILBs, have a lower CRI (typically in the 70s-90s)[4] resulting in a lower quality of light. By improving the efficiency of ILBs through better spectral control of the emission spectrum high performance lighting with perfect CRI, competitive with LEDs, could become a reality.

Improving the efficiency of ILBs is typically achieved by reducing infrared emission by surrounding the emitter with selective cold-side filters that transmit visible light but reflect infrared radiation back to the emitter. This approach reduces emission at infrared wavelengths while maintaining light emission at visible wavelengths where the human eye is sensitive. Extensive work has been published in the literature since it was first introduced in 1912[5]. Different types of optical filters were proposed such as silver films with TiO_2 antireflection coatings[6–10], multilayer dielectric films (Ta_2O_5-SiO_2[11–17] or TiO_2-SiO_2[18]), indium tin oxide (ITO) films[19] and metallic photonic crystals[20]. Ta_2O_5-SiO_2 multilayer films were found to offer the highest temperature stability and performance (luminous efficiency and CRI) for their application in ILBs. Several

*aleroy@mit.edu; phone +1-617-715-4044;

bulb or filter geometries such as cylindrical[5,11–13,17,18,20], spherical[6–10,19,21,22], ellipsoidal[10,14,15] and planar[16] were also explored to maximize the amount of infrared radiation recycled back to the emitter, minimize hot-spots on the emitter and reduce fabrication complexity. Although extensive literature has been published on infrared recycling for ILBs, only limited energy savings (maximum experimentally demonstrated energy savings of 51% compared to traditional ILBs[7]) has been achieved because of non-idealities in the filter, emitter and geometrical alignment.

In this work, we first model the role of non-idealities in the filter and emitter optical properties as well as in the view factor between the emitter and filter for a planar system[16]. A planar system, presented in Section 3.1, is used throughout this work as it allows for easier fabrication of the emitter and filter. Based on the results of this analysis, we propose a novel approach to improve the luminous efficiency of the incandescent light source by using selective emitters and filters, and validate it with theoretical and experimental results. Finally, we discuss challenges and future directions to achieve high performance and long-lasting incandescent lighting with the current planar geometry.

2. ROLE OF NON-IDEALITIES ON THE PERFORMANCE OF INCANDESCENT LIGHT BULBS WITH INFRARED FILTERS

We have developed a model to quantify the emission spectrum of the light source for a system featuring a planar emitter and filter separated by a spacing S. We find the effective emissivity of the system ε_{eff}[16] by accounting for reflections between the emitter and the filter, transmission through the filter and emission through the side gaps:

$$\epsilon_{eff} = \epsilon \left[\frac{FT + (1-F)(1+FR)}{1 - F^2 R(1-\epsilon)} \right] \tag{1}$$

where ε is the emissivity of the emitter, F is the view factor between the emitter and the filter, and R and T represent reflectivity and transmissivity of the filters respectively. The luminous efficiency η of the light source can then be calculated by weighting the emission spectrum with the human eye sensitivity curve $V(\lambda)$[3] and dividing by the total power consumption. For simplicity, only the total emissive power is considered for the total power consumption in the definition of the luminous efficiency.

$$\eta = \frac{\int_0^\infty \epsilon_{eff}(\lambda, T) E_b(\lambda, T) V(\lambda) d\lambda}{\int_0^\infty \epsilon_{eff}(\lambda, T) E_b(\lambda, T) d\lambda} \tag{2}$$

Equations (1) and (2) are used in the following sections to evaluate the influence of non-idealities in the filter, emitter and geometry (view factor) on the luminous efficiency of the system.

2.1 Non-idealities in the filter (R, T)

We first investigate the influence of non-idealities in the optical properties of the filter on the luminous efficiency (Figure 1). We model a system consisting of a tungsten emitter at 2800 K coupled with a filter of reflectivity R_{IR} in the infrared and transmissivity T_{VIS} in the visible. Absorption in the filter is assumed to be negligible and a view factor $F = 0.95$ is imposed between the emitter and the filter.
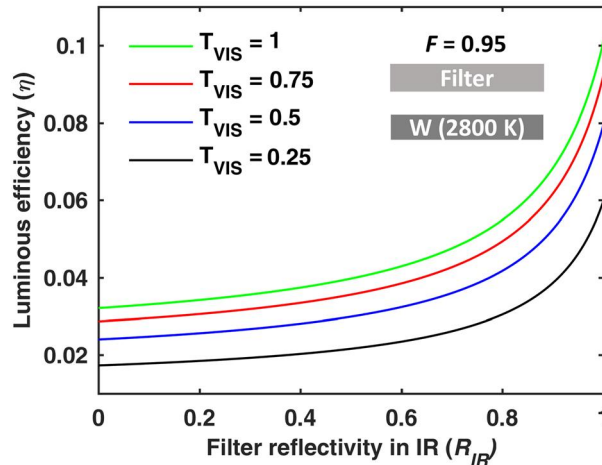
Figure 1. Influence of non-idealities in the filter (reflectivity R_{IR} in the infrared and transmissivity T_{VIS} in the visible) on the luminous efficiency of the light source. The tungsten emitter at 2800 K is radiatively coupled to the filter with a view factor $F = 0.95$.

As shown in Figure 1, increasing R_{IR} increases the luminous efficiency due to an increase in the infrared radiation reflected back to the emitter by the filter. Similarly, as we increase T_{VIS}, more visible light is transmitted through the filters which translates to higher luminous efficiency. However, we find that the maximum luminous efficiency is only 10.1% when using an ideal filter (i.e., $R_{IR} = 1$; $T_{VIS} = 1$), far from the theoretical maximum of 39.6% for a blackbody at a similar temperature truncated to the visible spectrum only (400-700 nm). This significant difference between the two cases arises because of the view factor $F < 1$ used in Figure 1, causing a fraction of the infrared radiation to escape the system through the gap between the emitter and filter after each reflection. While the optical properties of the filter can be optimized, we show that only limited luminous efficiencies can be achieved with a typical tungsten emitter and view factor.

2.2 Non-idealities in the emitter (ε)

Next, we look at the influence of non-idealities in the emitter on the performance of a light source. More specifically, we show in Figure 2 the influence of the visible (ε_{VIS}) and infrared (ε_{IR}) emissivity of an emitter with no filters on the luminous efficiency. Low emissivity in the infrared leads to higher efficiency due to smaller emission at undesirable wavelengths. However, higher emissivity in the visible allows for more visible light output at a same emitter temperature, thus higher luminous efficiencies. Figure 2 shows that very high luminous efficiencies can be achieved using a well-designed selective emitter. However, challenges associated with reducing ε_{IR} and thermal stability at incandescent temperatures make the use of a selective emitter alone impractical.
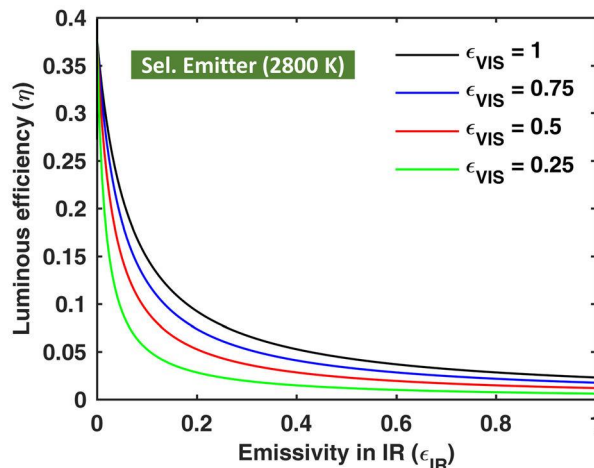

Figure 2. Influence of the emitter emissivity in the visible (ε_{VIS}) and infrared (ε_{IR}) at 2800 K on its luminous efficiency.

2.3 Non-idealities in the view factor (F)

Finally, we demonstrate the influence of view factor between the thermal emitter and filter on the luminous efficiency of the system. We show in Figure 3(a) the view factor F as a function of spacing between the emitter and filter, both of size 6 mm x 10 mm. For reference, the size of the emitter is equivalent to a 120 W ILB in terms of emitted lumens. In practice, it is difficult to achieve $F > 0.95$ (or spacing $< \sim 100$ μm) because of emitter sagging and deformation that can result in the emitter contacting the filter.

We plot in Figure 3(b) the luminous efficiency of a tungsten emitter coupled with an ideal filter ($T_{VIS} = 1; R_{IR} = 1$) as a function of view factor. We show that most gains in efficiency occur for $F > 0.95$ and that the maximum luminous efficiency occurring for $F \leq 0.95$ with an ideal filter is limited to 10.1%, far from the theoretical maximum of 39.6 % ($F = 1$). Because tungsten has a relatively low emissivity in the infrared at incandescent temperatures (~ 0.3), over 16 reflections between the emitter and an ideal filter will occur before 95% of the infrared radiation is reabsorbed by the emitter, thus highlighting the importance of the view factor on the luminous efficiency. Since near-perfect view factor is difficult to achieve, a different approach to what has previously been done (tungsten emitter surrounded with cold-side filters) should be explored if luminous efficiencies competitive with LEDs are to be achieved.
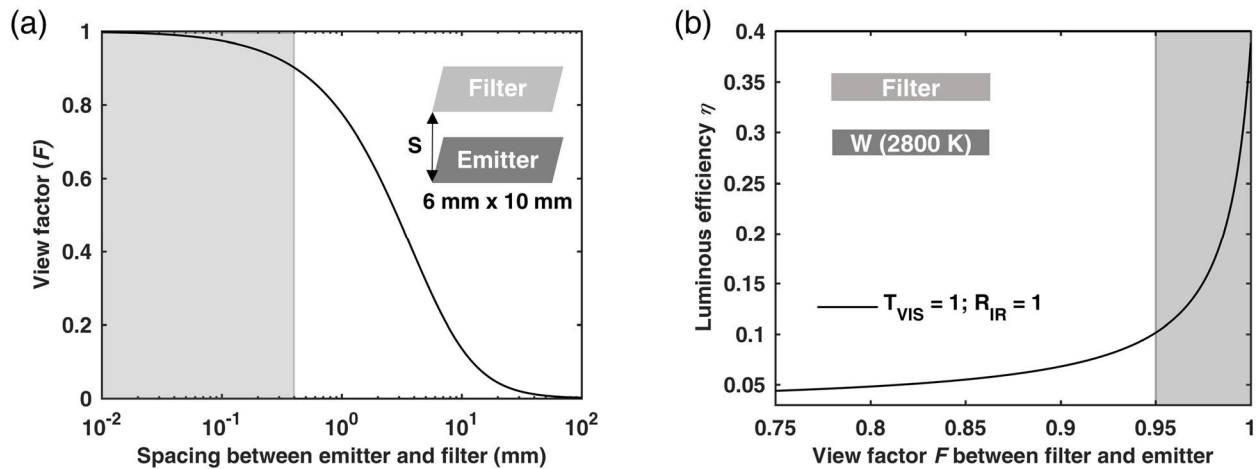

Figure 3. (a) View factor as a function of emitter-filter spacing for a 120 W ILB equivalent emitter size (6 mm x 10 mm). (b) Luminous efficiency as a function of view factor for a tungsten emitter combined with an ideal filter ($T_{VIS} = 1; R_{IR} = 1$). Most gains in efficiency occur at $F > 0.95$.

2.4 Combined selective emitter and filters

One approach that could minimize the effects of non-idealities in the filter properties and view factor could be to combine a selective emitter with the filter. We demonstrate in Figure 4 the luminous efficiency of a selective emitter coupled with a non-ideal filter ($R_{IR} = 0.9$ and $T_{VIS} = 1$) at a view factor of $F = 0.95$ as a function of the selective emitter optical properties ε_{VIS} and ε_{IR}. We observe that even with a non-ideal view factor and filter, we can achieve luminous efficiencies of up to 39.6%, which is six times higher than achieved for a tungsten emitter (W; 6.5%). We also show that if we increase the emissivity in the visible ε_{VIS} of the typical tungsten emitter (W) to $\varepsilon_{VIS} = 1$ (SE; e.g., by coating the tungsten with an antireflection coating) while maintaining ε_{IR} constant, we can nearly double the luminous efficiency from 6.5% to 12.5%. By reducing ε_{IR} or increasing ε_{VIS} of the emitter compared to a tungsten emitter, we have shown that important gains in efficiency could be achieved even with a non-ideal view factor and filter. In the next section, we experimentally demonstrate the benefits of this approach.
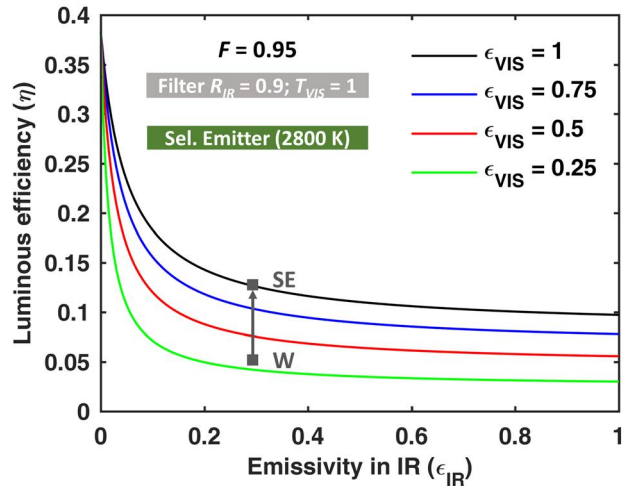
Figure 4. Luminous efficiency of a selective emitter coupled with a filter ($R_{IR} = 0.9$ and $T_{VIS} = 1$) as a function of ε_{VIS} and ε_{IR}.

3. COMBINING SELECTIVE EMITTER AND FILTERS

3.1 Experimental procedure

To validate our proposed approach, we experimentally compare the emission spectrum and the power consumption of a tungsten emitter and a selective emitter, combined with the same nanophotonic filter (Figure 5(a)) with an equal view factor.

For simplicity, our selective emitter was made by coating a tungsten emitter with a high-temperature-stable[23–25] HfO_2 antireflection coating to increase its emissivity in the visible spectrum as was proposed in Figure 4. An optimized film thickness of around 55 nm was determined using Fresnel equations at normal incidence to maximize luminous efficiency. The optical properties of the bare tungsten emitter and the selective emitter are shown in Figure 5(b), measured using a UV-visible spectrophotometer (Carry 6000i).

The emitter was sandwiched between a pair of planar nanophotonic filters which were held by copper supports for efficient heat dissipation and precise alignment (Figure 5(c)). The emitter was fixed to custom molybdenum electrical feedthroughs for high temperature resistive heating. The whole assembly was located inside a bell jar vacuum chamber (Kurt J. Lesker) and maintained at pressures <10^{-6} Torr to minimize contaminants such as residual water vapor that could react with the emitter at high temperature. Outside the vacuum chamber, a spectrometer (USB4000 Ocean Optics) was used to measure the emission spectrum of the light source. A power supply (E3632A Agilent) was used to resistively heat the emitter and a multimeter (2000 Multimeter Keithley) measured the emitter resistance using a four-point measurement technique.

A COMSOL model was developed to correlate the measured emitter resistance to its temperature. Inputs to the COMSOL model were the emitter geometry and temperature dependent tungsten total hemispherical emissivity and electrical resistivity.
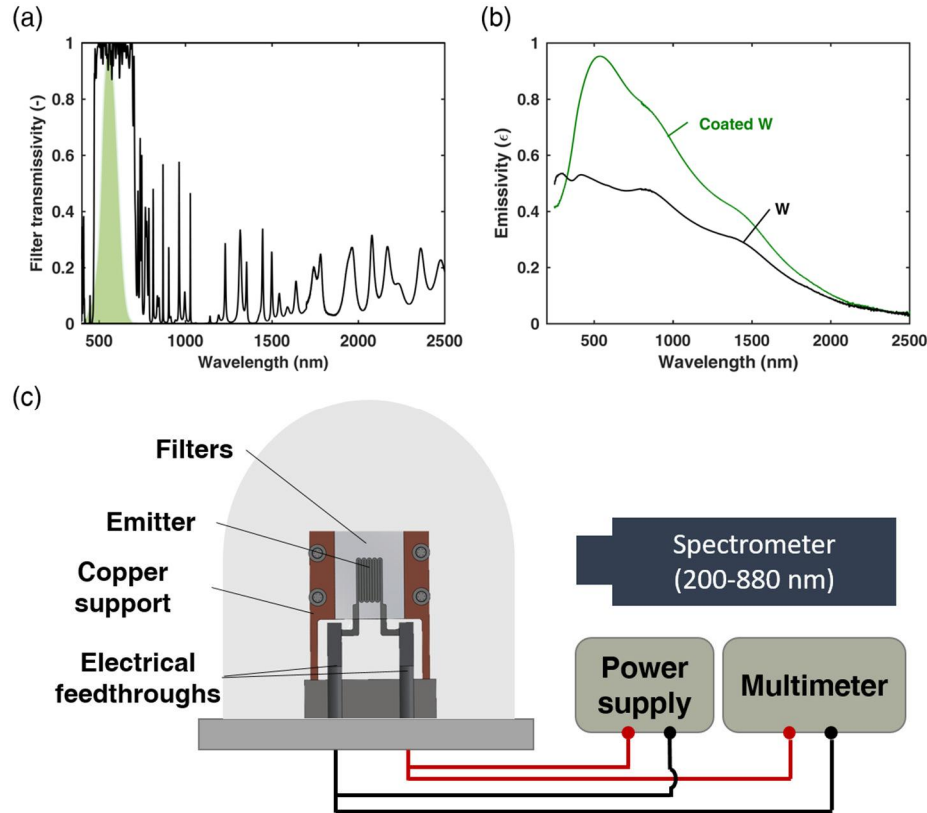
Figure 5. Details of experimental setup. (a) Optical properties of the nanophotonic filter[16] consisting of 90 alternating layers of Ta_2O_5 and SiO_2 on a 1 mm thick fused silica substrate. (b) Emissivity of the tungsten emitter and the selective emitter (HfO_2 coated tungsten). (c) Main components of experimental setup.

3.2 Results

The experimental setup allows us to compare the emission spectrum and power consumption of three different configurations (tungsten emitter only, *W*; tungsten emitter with filters, *W + Filters*; selective emitter with filters, *Coated W + Filters*) and compare their performance.

We first measure the emission spectrum of the three different systems to evaluate the relative improvements of adding a selective filter and emitter. In Figure 6, we show the spectral intensity ratio *r* of each system where the emission spectrum of a bare tungsten emitter (*W*) is the reference. Consequently, the spectral intensity ratio of *W* is represented as a line at *r* = 1. We observe that adding filters to a tungsten emitter (*W + Filters*) can significantly suppress the emission in the near infrared without any reduction in the visible light emission where the human eye is sensitive. In our proposed approach, we further show that by replacing the tungsten emitter with our selective emitter (*Coated W + Filters*), we maintain the low emission in the near infrared, but the emission of visible light is nearly doubled due to the higher emissivity of the emitter at visible wavelengths. By using an appropriately designed selective emitter, these results suggest that higher luminous efficiencies can be achieved.
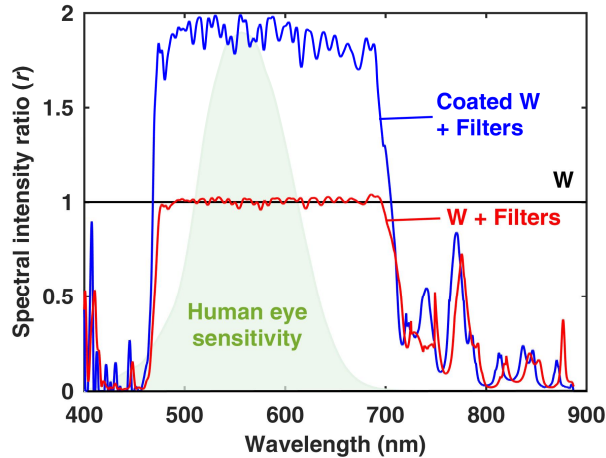
Figure 6. Experimental spectral intensity ratio *r* of three different systems – bare tungsten emitter (*W*), tungsten emitter with filters (*W + Filters*) and HfO$_2$ coated tungsten emitter with filters (*Coated W + Filters*), taken with respect to the emission spectrum of a bare tungsten emitter. Spectra were measured at temperatures between 1800 K and 2200 K to maximize the emission at short wavelengths. An average experimental error (instrumental and precision error) of 0.04 on the spectral intensity ratio was calculated for the range of wavelengths plotted.

Next, we compare in Figure 7 the power consumption of the emitter as a function of temperature for the three systems to evaluate the improvement in efficiency when using a selective filter and emitter. We account for the difference in visible light emission, demonstrated in Figure 6, by normalizing the power consumption by the number of lumens emitted from the light source. Up to 50% energy savings can be achieved by adding filters to the tungsten emitter (*W + Filters*), in comparison to the reference case of a tungsten emitter (*W*). However, when using the HfO$_2$ coated tungsten emitter with the same filters (*Coated W + Filters*), up to 67% energy savings are demonstrated, which represents a 34% improvement over the previous approach to use a tungsten emitter with selective filters (*W + Filters*). By combining a simple selective emitter with selective filters, we have experimentally demonstrated important improvements in efficiency over previous approaches (*W* and *W + Filters*), thus validating our approach and modeling.
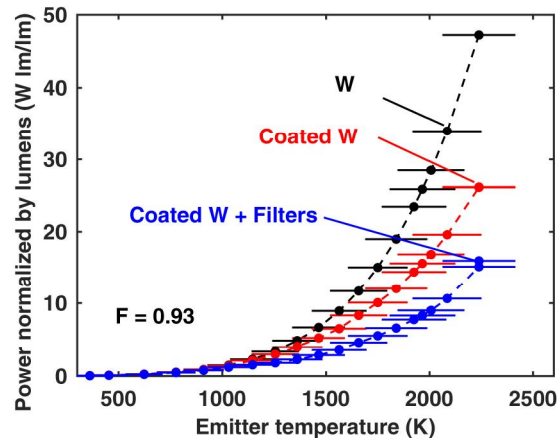

Figure 7. Comparison of the power consumption as a function of emitter temperature for the three systems studied (*W, W + Filters, Coated W + Filters*). The power consumption is normalized by the number of emitted lumens to account for the different visible emissivity of the emitters.

While the experimental demonstration showed that using a simple selective emitter could lead to significant energy savings, even better performance could be achieved by using better selective emitters and filters. Figure 4 showed that using better selective emitters and filters, luminous efficiencies surpassing that of current LEDs while maintaining high CRI is possible. The development of high performance selective emitters could pave the way for high efficiency incandescent lighting competitive with LEDs. However, several challenges such as thermal stability of the emitter and

filter as well as evaporation of the emitter on the filter need to be addressed before we can achieve a high performance and long-lasting incandescent lighting with selective emitter and filters.

4. CHALLENGES AND FUTURE DIRECTIONS

4.1 Temperature stability of the filter

Due to the high radiative heat flux at the filter due to the thermal emission from the emitter ($\sim 10^6$ W/m² at 2800 K), any absorption within the filter will cause its temperature to rise. We can also expect that owing to the planar geometry of the studied system, the filter temperature will increase as the view factor is increased (i.e., when the spacing between the emitter and the filter is decreased), because of a higher radiative heat flux on the filter. While we want to maximize the view factor to maximize the luminous efficiency of the system, it is important to prevent thermal degradation in the filter. To ensure thermal stability throughout the lifetime of the light source, it is recommended that the multilayer interference filter (alternating layers of Ta_2O_5 and SiO_2) temperature should be maintained below 800 °C[12,15,17]. In this section, we investigate the influence of this maximum filter temperature on the performance of the system.

In order to estimate the filter temperature as a function of the emitter temperature and view factor, we developed a COMSOL model replicating our experimental setup illustrated in Figure 5(c). Solving for the maximum filter temperature as a function of tungsten emitter temperature and view factor, we estimated the maximum allowable view factor to maintain the maximum filter temperature below 800 °C. Figure 8 shows these results (red curve) plotted on top of a contour plot of the luminous efficiency as a function of emitter temperature and view factor. These results show that a maximum luminous efficiency of 4.8% can be achieved for tungsten emitter temperatures ≤ 3000 K while maintaining the maximum filter temperature below 800 °C. This represents only a slight improvement over a bare tungsten emitter at 3000 K, which has a luminous efficiency of 4.2%.
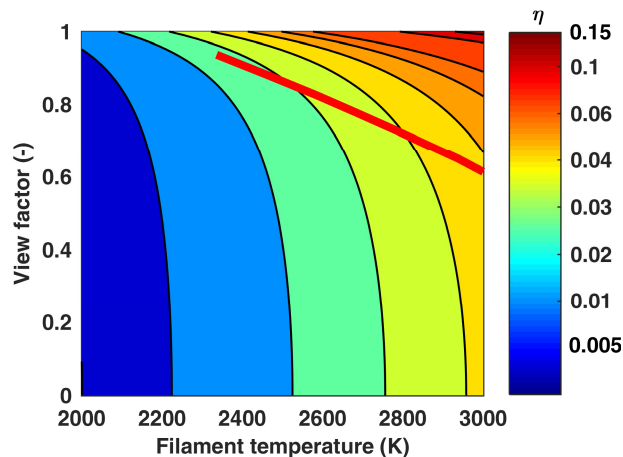

Figure 8. Maximum efficiency as a function of emitter temperature when respecting the maximum filter temperature.

While in theory we could achieve an efficiency of around 14% with a tungsten emitter coupled with the fabricated nanophotonic filter at $F = 1$, the high-temperature stability of the filter limits the luminous efficiency. Better thermal management of the filter in this current planar geometry is necessary to achieve a high efficiency and long-lasting light source. The use of better selective emitters which can operate efficiently at lower temperatures along with thinner fused silica substrates for the filter could also help decrease the absorbed radiative heat flux at the filter and increase its thermal stability.

4.2 Temperature stability of the selective emitter

As was suggested in Figure 8, higher emitter temperatures lead to higher luminous efficiencies since a greater portion of the blackbody spectrum is at visible wavelengths (400-700 nm). However, in practice, thermal degradation of the selective

emitter can also occur at high temperatures, significantly affecting the lifetime of the light source, and altering the optical properties of the emitter.

In our experimentations with the HfO_2 coated tungsten emitter, thermal degradation and evaporation of the thin film occurred at high temperatures, limiting the maximum temperature of the experiments. This thermal degradation of the thin film was further investigated by maintaining a HfO_2 coated tungsten emitter (Figure 9(a)) at 1800 K for 24 h (Figure 9(b)) and then at 2850 K for 1 min (Figure 9(c)). During this test, the degradation of the HfO_2 thin film was accompanied by a slow shift towards longer wavelengths and resulted in an increase in power consumption at constant temperature. Higher magnification optical images of the HfO_2 surface after high-temperature exposure at 1800 K for 24 h are depicted in Figure 9(d), which shows a granular structure on the micron length scale likely caused by a change in the HfO_2 phase or by an increase in crystallite size. High temperature stability of the emitter is yet another challenge to achieving long-lasting and high performance incandescent lighting, and requires significant research and development.
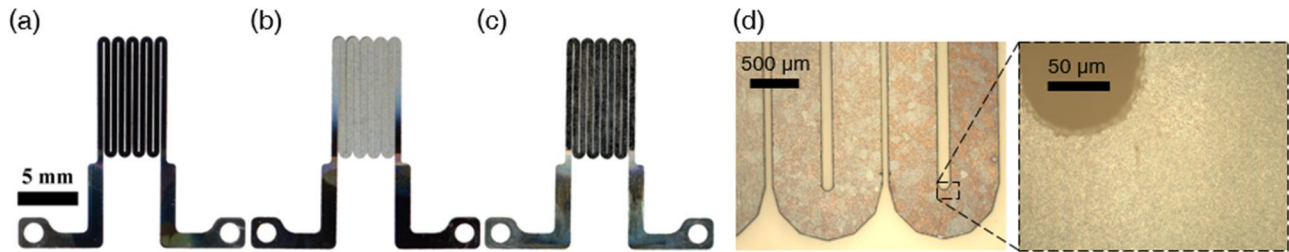

Figure 9. Thermal degradation of the HfO_2 thin film deposited on the tungsten emitter: (a) as deposited (b) after 24 h at 1800 K (c) after 1 min at 2850 K. (d) Microscope images of the HfO_2 thin film on a tungsten emitter after 24 h at 1800 K. Macroscopic changes in colors across the surface of the emitter are observed while a granular structure (micron length scale) is observed at higher magnifications.

4.3 Evaporation of the emitter

Beyond the thermal stability of the emitter, the evaporation of the emitter on the filter can also severely degrade the performance of the light source. This evaporation of the emitter can cause darkening of the optical filter, leading to a reduced transmittance and increased absorption resulting in lower visible light output and higher filter temperature.

Taking a tungsten emitter as an example, it is estimated that a 67% reduction in transmittance of the filter can occur due to the deposition of an 8 nm thick layer of tungsten. Setting this deposition as a failure criterion, we calculate and plot in Figure 10 the time until this criterion is met for a range of emitter temperatures[26–28]. For comparison, the typical lifetime of ILBs and LEDs is also included. As shown in Figure 10, significant evaporation of the emitter in vacuum occurs at high temperatures, severely limiting the lifetime of the device down to only minutes. As is usually done in ILBs, an inert gas such as argon can be added to reduce the evaporation rate[29,30]. However, even with argon gas, Figure 10 shows that our current system does not last as long as a typical ILBs with similar gas and emitter material. This difference can be attributed to the area ratio between the emitter and the glass or filter. This area ratio is estimated to be about two orders of magnitudes higher in our planar configuration compared than in a traditional ILB with a small coiled-coil filament surrounded by a much larger bulb. This higher area ratio means that the evaporated tungsten is concentrated on a smaller area on the filter, leading to faster filter darkening. Due to the evaporation of the emitter and the high area ratio between the emitter and filter, we have shown that the lifetime of the light source can be very short for the range of temperatures of interest.

For the planar geometry tested, evaporation of the emitter and the high area ratio between the emitter and filter limit the lifetime of the device due to filter darkening. Although an inert gas can help reduce the evaporation rate, its effect is limited at close to atmospheric pressure. In addition, the inert gas introduces an additional heat transfer pathway, which could cause thermal degradation of the filters. Finally, the use of other materials to improve the optical selectivity of the emitter will lead to even higher evaporation rates and shorter lifetimes because of higher vapor pressures than tungsten.
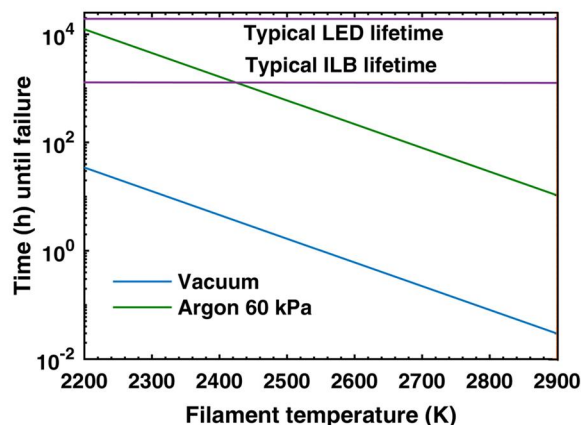
Figure 10. Estimated lifetime of our experimental planar light source based on the tungsten emitter evaporation on the filter for a range of emitter temperatures. Increased lifetime can be achieved by adding an inert gas such as argon. Lifetime of our planar system is lower than typical ILBs due to higher area ratio between the emitter and filter. While higher emitter temperatures are desirable to maximize the emission in the visible, evaporation of the emitter limits the maximum temperature in practice.

5. CONCLUSIONS

In summary, we studied the role of non-idealities in the optical properties of the filter and emitter as well as view factor between the emitter and filter on the luminous efficiency of the light source. Our modeling work suggests that at view factors typically observed in practice the maximum luminous efficiency is limited to below 10.1%, even with a perfect filter. We showed that by combining selective emitter and filter, significantly higher luminous efficiencies could be achieved, even with non-ideal view factors and filters. This was demonstrated using experiments which showed energy savings of up to 67% compared to a bare tungsten emitter. Finally, we discussed several challenges such as filter and emitter thermal stability and emitter evaporation that should be addressed to achieve high performance incandescent lighting with the current geometry and design. The development of high temperature stable thermal emitters proposed in this work, along with adequate thermal management of the filters, could lead to a next generation of high performance light sources.

ACKNOWLEDGMENTS

REFERENCES

[1]   Energy Information Administration - EIA - Official Energy Statistics from the U.S. Government., "How much electricity is used for lighting in the United States? - FAQ - U.S. Energy Information Administration (EIA)," 2017, <https://www.eia.gov/tools/faqs/faq.php?id=99&t=3> (12 June 2017).

[2]   Woodward, M.., McNary, B., "American households use a variety of lightbulbs as CFL and LED adoption increases," U.S. Energy Inf. Adm., 2017, <https://www.eia.gov/todayinenergy/detail.php?id=31112> (12 May 2017).

[3]   Sharpe, L. T., Stockman, A., Jagla, W.., Jägle, H., "A luminous efficiency function, VD65* (λ), for daylight adaptation: A correction," Color Res. Appl. **36**(1), 42–46 (2011).

[4]   U.S. Department of Energy - Office of Energy Efficiency & Renewable Energy., "Lighting Basics | Department of Energy," 2013, <https://energy.gov/eere/energybasics/articles/lighting-basics> (1 March 2017).

[5]   Hoffman, S. O., "Production of light," 1,043,008, 4, United States Patent Office, San Francisco, United States (1912).

[6]   Brett, J., Fontana, R. P., Walsh, P. J.., Spura, S. A., "Radiation-conserving incandescent lamps," J. Illum. Eng. Soc. **9**(4), 197- (1980).

[7]   Brett, J.; Fontana, R.; Walsh, P.; Spura, S.; Parascandola, L.; Thouret, W.; Thorington, L., "Development of high energy-conserving incandescent lamps," J. Illum. Eng. Soc. **10**(4), 214–218 (1981).

[8]   Spura, S. A., Fontana, R., Parascandola, L. J., Thouret, W. E.., Thorington, L., Thin Silver Film Coating for Increased Lamp Efficiency, Precious Met. **2**, Pergamon Press Canada Ltd. (1982).

[9]   Yoldas, B. E.., O'Keefe, T., "Deposition of optically transparent IR reflective coatings on glass," Appl. Opt. **23**(20), 3638–3643 (1984).

[10]   Fontana, R. P., Goldstein, I. S., Thorington, L.., Howson, R. P., "The design, construction and performance of an incandescent light source with a transparent heat mirror," CIE J. **6**(1), 11–16 (1987).

[11]   Hoegler, L. E. ; McGowan, T. K., "Practical high efficiency tungsten-halogen lamps using IR reflecting films," J. Illum. Eng. Soc. **14**(1), 165- (1984).

[12]   Rancourt, J. D.., Martin, Jr., R. L., "High temperature lamp coatings," Opt. Thin Film. II New Dev., R. I. Seddon, Ed., 185–191 (1986).

[13]   Bergman, R. S., "Halogen-IR lamp development: A system approach," J. Illum. Eng. Soc. **20**(2), 10 (1991).

[14]   Omata, Y., Hashimoto, N., Kawagoe, S., Suemitsu, T.., Yokoyama, M., "Sputtering deposition of infra-red reflecting films on ellipsoidal bulbs of energy saving lamps," Light. Res. Technol. **34**(2), 111–119 (2002).

[15]   General Electric., "ConstantColor TM Precise TM IR Energy efficient low voltage dichroic mirror halogen reflector lamps," GE Light. Datasheet, 2010, <http://www.gelighting.com/LightingWeb/aus/images/ge-hal-mr16-precise-constant-color-ir-datasheet_tcm284-46208.pdf> (3 January 2017).

[16]   Ilic, O., Bermel, P., Chen, G., Joannopoulos, J. D., Celanovic, I.., Soljačić, M., "Tailoring high-temperature radiation and the resurrection of the incandescent source," Nat. Nanotechnol. **11**(4), 320–324 (2016).

[17]   Martin, Jr., R. L.., Rancourt, J. D., "Optical tantalum pentoxide coatings for high temperature applications," US 4663557 A, United States (1982).

[18]   Honda, K., Ishizaki, A., Yuge, Y.., Saitoh, T., "Infrared Reflective Filter and Its Applications," Proc. Soc. Photo-Optical Instrum. Eng. **428**, 29–31 (1983).

[19]   Kostlin, H. .., Frank, G., "Thin-film reflection filters," Philips Tech. Rev. **41**(7), 225–238 (1983).

[20]   Kim, Y. S., Lin, S. Y., Chang, A. S. P., Lee, J. H.., Ho, K. M., "Analysis of photon recycling using metallic photonic crystal," J. Appl. Phys. **102**(6) (2007).

[21]   Hoffman, S. O., "Lamp," 1,425,967, 3, United States Patent Office, United States (1922).

[22]   Studer, F. J.., Cusano, D. A., "Titanium dioxide films as selective reflectaors of the near-infrared," J. Opt. Soc. Am. **43**(6), 522 (1953).

[23]   Rinnerbauer, V., Lenert, A., Bierman, D. M., Yeng, Y. X., Chan, W. R., Geil, R. D., Senkevich, J. J., Joannopoulos, J. D., Wang, E. N., et al., "Metallic Photonic Crystal Absorber-Emitter for Efficient Spectral Control in High-Temperature Solar Thermophotovoltaics," Adv. Energy Mater. **4**(12), 1400334 (2014).

[24]   Stelmakh, V., Rinnerbauer, V., Geil, R. D., Aimone, P. R., Senkevich, J. J., Joannopoulos, J. D., Soljačić, M.., Celanovic, I., "High-temperature tantalum tungsten alloy photonic crystals: Stability, optical properties, and fabrication," Appl. Phys. Lett. **103**(12) (2013).

[25]   Chou, J. B., Yeng, Y. X., Lee, Y. E., Lenert, A., Rinnerbauer, V., Celanovic, I., Soljačić, M., Fang, N. X., Wang, E. N., et al., "Enabling ideal selective solar absorption with 2D metallic dielectric photonic crystals," Adv. Mater. **26**(47), 8041–8045 (2014).

[26]   Szwarc, R., Plante, E. R.., Diamond, J. J., "Vapor pressure and heat of sublimation of tungsten," J. Res. Natl. Bur. Stand. Sect. A Phys. Chem. **69A**(5), 417 (1965).

[27]   Plante, E. R.., Sessoms, A. B., "Vapor pressure and heat of sublimation of tungsten," Phys. Chem. **77A**, 237–242 (1973).

[28]   Zwikker, C., "Physische eigenschappen van wolfraam bij hooge temperaturen," Proc. R. Netherlands Acad. Arts Sci. **5**(249) (1925).

[29]   Fromm, E., "Reduction of Metal Evaporation Losses by Inert Gas Atmospheres," Metall. Trans. **9**(December), 1835–1838 (1978).

[30]   Harvey, F. J., "Rate of vaporatization of tungsten in argon," Metall. Trans. **3**(11), 2973–2978 (1972).